Structural Engineering and Mechanics, *Vol. 49, No. 1 (2014) 41-64*
DOI: http://dx.doi.org/10.12989/sem.2014.49.1.041

Stochastic analysis of elastic wave and second sound propagation in media with Gaussian uncertainty in mechanical properties using a stochastic hybrid mesh-free method

Seyed Mahmoud Hosseini*[1] and Farzad Shahabian[2]

[1]*Industrial Engineering Department, Faculty of Engineering, Ferdowsi University of Mashhad, PO Box: 91775-1111, Mashhad, Iran*
[2]*Civil Engineering Department, Faculty of Engineering, Ferdowsi University of Mashhad, PO Box: 91775-1111, Mashhad, Iran*

(Received October 22, 2012, Revised October 15, 2013, Accepted December 9, 2013)

Abstract. The main objective of this article is the exploitation of a stochastic hybrid mesh-free method based on stochastic generalized finite difference (SGFD), Newmark finite difference (NFD) methods and Monte Carlo simulation for thermoelastic wave propagation and coupled thermoelasticity analysis based on GN theory (without energy dissipation). A thick hollow cylinder with Gaussian uncertainty in mechanical properties is considered as an analyzed domain for the problem. The effects of uncertainty in mechanical properties with various coefficients of variations on thermo-elastic wave propagation are studied in details. Also, the time histories and distribution on thickness of cylinder of maximum, mean and variance values of temperature and radial displacement are studied for various coefficients of variations (COVs).

Keywords: second sound; stochastic generalized finite difference (SGFD) method; thermal shock; coupled thermoelasticity; Gaussian uncertainty

1. Introduction

Uncertainty in some thermo-elasticity parameters such as mechanical properties has a significant effect on transient behavior of displacement and temperature fields and also on thermo-elastic stresses in structures subjected to transient or thermal shock loadings. The reliability and safety evaluations of displacement and temperature fields in structures should be stochastically studied considering uncertainty in some parameters such as mechanical properties. To assess the thermo-elastic wave propagation and transient behaviors of displacement and temperature fields in structures from engineering perspective, the coupled thermo-elasticity governing equations should be analyzed using mechanical properties with Gaussian or other distributions.

Recently, some works were presented in this field. The statistics (i.e., mean and variance) of temperature and thermal stress were analytically obtained in functionally graded material (FGM) plates with uncertainties in the thermal conductivity and coefficient of linear thermal expansion

*Corresponding author, Ph.D., E-mail: sm_hosseini@um.ac.ir
MSC No. 74J05, 74F05, 65C30, 82C31

http://www.techno-press.org/?journal=sem&subpage=8 ISSN: 1225-4568 (Print), 1598-6217 (Online)

(Chiba *et al*. 2008). They assumed the FG plate to have arbitrary nonhomogeneous thermal and mechanical properties through the entire thickness of plate and were subjected to deterministic convective heating. In another work, the second-order statistics (i.e., mean and standard deviation) of the temperature and thermal stresses were evaluated in an axisymmetrically heated functionally graded annular disc of variable thickness with spatially random heat transfer coefficients (HTCs) on the major surfaces of the disc (Chiba 2009). This annular disc was assumed to have arbitrary variations in the HTCs and material composition along the radial direction only. Stochastic analysis of generalized coupled thermoelasticity with one relaxation time in a half space was carried out considering stochastic boundary conditions, which were white noise (Sherief *et al*. 2013).

The uncoupled theory of thermo-elasticity is not a realistic approach for thermo-elasticity analysis, especially for structures under shock loading. To simulate the finite speed thermal wave propagation and also the real physical behaviors in high strain rate and highly varying thermal boundary conditions, some theories have been presented to simulate the mutual dependency between temperature and displacements. In thermo-elasticity, these approaches are usually indicated as coupled thermo-elasticity theories. Green and Naghdi presented a theory in which the finite speed of thermal wave was simulated and the propagation of thermo-elastic waves was modeled in a domain with high rate excitation (Green *et al*. 1993, Chandrasekharaiah 1998). Their theory has been called as GN theory in coupled thermo-elasticity.

There are some literatures in which the coupled thermo-elasticity analysis has been carried out by researchers. Melnik studied on the properties of discrete approximations for mathematical models of coupled thermoelasticity in the stress-temperature formulation (Melnik 2001). The locally transversal linearization (LTL) technique with the numerical inverse Laplace transform method were successfully used to solve GN coupled thermo-elasticity in an annulus (Taheri *et al*. 2005). To study on coupled thermoelasticity of isotropic and homogeneous hollow spheres and cylinders based on LS, GL and GN theories, Bagri *et al*. presented a unified formulation for all theories (Bagri *et al*. 2007a). Also, they (Bagri *et al*. 2007b) developed their unified formulation for functionally graded cylinders and used the transfinite element method and numerical inverse Laplace technique to solve it.

Hosseini *et al*. used the hybrid numerical method based on Galerkin finite element (GFE) and Newmark finite difference (NFD) methods to analyze the GN coupled thermo-elasticity in a functionally graded (FG) thick hollow cylinder with infinite (1D) and finite (2D) length (Hosseini *et al*. 2008, Hosseini 2009). In their works, the FG cylinder was divided through radial direction to many isotropic sub-cylinders to simulate the FGM features. In other works, the GN coupled thermo-elasticity analysis was carried out with considering uncertainty in constitutive mechanical properties of FGM (Hosseini *et al*. 2011a, b). The random field of mechanical properties was generated using Monte Carlo simulation. The hybrid numerical method based on GFE (Galerkin finite element) and NFD (Newmark finite difference) methods were employed to solve the GN governing equations. In another work, Hosseini *et al*. developed the application of meshless local Petrov-Galerkin (MLPG) method in GN coupled thermo-elasticity of functionally graded thick hollow cylinder subjected to thermal shock loading (Hosseini 2011c), also solving a similar problem in stochastic field by considering uncertainty in constitutive mechanical properties of FGMs (Hosseini 2011d).

There is another method without any mesh generation, which is called generalized finite difference (GFD) method, to solve the partial differential equations. Benito *et al*. developed application of the GFD method in parabolic and hyperbolic differential equations and also they

analyzed the possibility of employing the GFD method over adaptive clouds of points progressively increasing the number of nodes (Benito *et al*. 2001, 2003). A procedure in GFD was given that can easily assure the quality of numerical results by obtaining the residual at each point (Gavete *et al*. 2003). Also, they compared the GFD method with another meshless method, so-called, element free Galerkin method (EFG). Benito *et al*. applied the GFDM to solve the parabolic and hyperbolic differential equations. In their research, some examples from two kinds of differential equations were solved (Benito *et al*. 2007).

In this article, a stochastic hybrid mesh-free method based on stochastic generalized finite difference (SGFD) method is exploited to analyze the GN coupled thermoelasticity in thick hollow cylinder with uncertainty in mechanical properties. The Gaussian distribution is considered to generate the random mechanical properties with various coefficients of variations (COVs). The thermoelastic wave propagation across thickness of cylinder have been studied for various values of COVs and also the time history of non-dimensional radial displacement and temperature are obtained for various points on thickness of cylinder. The mean, maximum and variance of non-dimensional displacement and temperature fields are studied in details for various times and COVs at several points on thickness. The presented stochastic hybrid mesh-free method shows a high capability to use in coupled thermoelasticity analysis.

2. Coupled thermoelasticity governing equations

Consider a thick hollow cylinder with inner radius r_{in} and outer radius r_{out}, which is subjected to thermal shock loading. To find the dynamic response of displacement field, the coupled thermoelasticity governing equations should be considered for the problem. One of the most important theories in coupled thermoelasticity is Green and Naghdi (GN) model of generalized coupled thermoelasticity (Green *et al*. 1993). The GN theory simulates the dependency between the temperature and displacement with and without energy dissipation, which are called type II and type III of GN theory. The type I is reduced to the classical heat conduction theory (based on the Fourier's law). The governing equations of GN theory without energy dissipation are given as

$$\nabla.\boldsymbol{\sigma} + \rho\mathbf{F} = \rho\ddot{\mathbf{u}} \tag{1}$$

$$c\ddot{T} + \gamma T_0 \nabla.\ddot{\mathbf{u}} = \rho\dot{g} + \nabla.\left(k^*\nabla T\right) \tag{2}$$

where u is the displacement vector, T is the temperature change with respect to the uniform reference temperature T_0, F is the external force and $\dot{g}$ is the external rate of supply of heat. Furthermore, ρ is the mass density, c is the specific heat, λ and μ are the Lame constants and

$$\gamma = (3\lambda + 2\mu)\beta^* \tag{3}$$

where β is the coefficient of volume expansion and k^* is a material constant characteristic of the GN theory. The dot over the symbol denotes time differentiation. Assuming linear elasticity, the stress field can be computed using the following equation

$$\sigma_{ij} = \delta_{ij}\left(\lambda\, u_{k,k} - \gamma T\right) + \mu\,(u_{i,j} + u_{j,i}) \tag{4}$$

The axi-symmetry and plane strain conditions are assumed for the problem. Consequently, the following relations are taken into account.

$$u_\theta = 0\,,\; u_z = 0\,,\; \sigma_{rr} = 2\,\mu\, u_{r,r} + \left(\lambda\, e - \gamma T\right)$$

$$\sigma_{\theta\theta} = 2\mu\, u_r / r + \left(\lambda\, e - \gamma T\right) \quad , \quad \sigma_{zz} = \lambda\, e - \gamma T, \tag{5}$$

$$\sigma_{r\theta} = \sigma_{rz} = \sigma_{z\theta} = 0 \tag{6}$$

where the term *e* is obtained as

$$e = u_{r,r} + u_r \big/ r \tag{7}$$

The governing Eqs. (1) and (2) can be rewritten as follows.

$$\mu\nabla^2\mathbf{u} + \left(\lambda + \mu\right)\nabla\mathrm{div}\,\mathbf{u} - \gamma\nabla T + \rho F = \rho\ddot{\mathbf{u}} \tag{8}$$

$$c\ddot{T} + \gamma T_0 \mathrm{div}\,\ddot{\mathbf{u}} = \rho\dot{g} + k^*\nabla^2 T \tag{9}$$

The F and $\dot{g}$ are considered to be zero in this work. To analyze the problem, we use the non-dimensional parameters as follows.

$$\bar{r} = \frac{r}{l},\; \bar{t} = \frac{v}{l}t,\; \bar{\mathbf{u}} = \frac{1}{l}\frac{\left(\lambda + 2\mu\right)}{\gamma T_0}\mathbf{u},\; \bar{T} = \frac{T}{T_0},\; \bar{\sigma}_r = \frac{\sigma_r}{\gamma T_0},\; \bar{\sigma}_\theta = \frac{\sigma_\theta}{\gamma T_0} \tag{10}$$

where l is a standard length (which can be assumed to be outer radius of cylinder for example) and v is a standard speed (which can be assumed to be the elastic wave propagation velocity in material of cylinder for example). The term T_0 stands for a certain value of temperature (for example environment temperature) and the terms λ and μ stand for Lame's constants. The governing equations, which are (1) and (2) can be rewritten by using nondimensional parameters

$$C_s{}^2\nabla^2\bar{\mathbf{u}} + \left(C_p{}^2 - C_s{}^2\right)\nabla\mathrm{div}\;\bar{\mathbf{u}} - C_p{}^2\nabla\bar{T} = \ddot{\bar{\mathbf{u}}} \tag{11}$$

$$C_T{}^2\nabla^2\bar{T} = \ddot{\bar{T}} + \varepsilon^*\mathrm{div}\,\ddot{\bar{\mathbf{u}}} \tag{12}$$

where

$$C_p{}^2 = \frac{\lambda + 2\mu}{\rho v^2}\;,\; C_T{}^2 = \frac{k^*}{cv^2}\;,\; C_s{}^2 = \frac{\mu}{\rho v^2}\;,\; \varepsilon^* = \frac{\gamma^2 T_0}{c\left(\lambda + 2\mu\right)} \tag{13}$$

The governing equations for axisymmetry and plane strain conditions can be obtained as follows

$$C_p{}^2 \frac{\partial^2 \bar{u}_r}{\partial \bar{r}^2} + C_p{}^2 \frac{1}{\bar{r}} \frac{\partial \bar{u}_r}{\partial \bar{r}} - \left(C_p{}^2 - C_s{}^2 \right) \frac{\bar{u}_r}{\bar{r}^2} - C_p{}^2 \frac{\partial \bar{T}}{\partial \bar{r}} = \ddot{u}_r \tag{14}$$

$$C_T{}^2 \left[\frac{\partial^2 \bar{T}}{\partial \bar{r}^2} + \frac{1}{\bar{r}} \frac{\partial \bar{T}}{\partial \bar{r}} \right] = \ddot{\bar{T}} + \varepsilon^* \left[\frac{\partial \ddot{\bar{u}}_r}{\partial \bar{r}} + \frac{\ddot{\bar{u}}_r}{\bar{r}} \right] \tag{15}$$

To study the effects of uncertainty in mechanical properties on dynamic behavior and thermoelastic waves, some random variables are replaced in the set of coupled equations. Uncertain mechanical properties are numerically generated with Gaussian distribution with different coefficients of variations using Monte Carlo simulation method. The mean values of random variables are considered to be equal with the deterministic values of mechanical properties. The symbol ~, which may be appeared above some parameters, stands for random variables. Consequently, the governing equations can be rewritten in random field as follows

$$\tilde{\mu} \nabla^2 \tilde{\mathbf{u}} + \left(\tilde{\lambda} + \tilde{\mu} \right) \nabla \mathrm{div}\, \tilde{\mathbf{u}} - \tilde{\gamma} \nabla \tilde{\theta} = \tilde{\rho} \ddot{\tilde{\mathbf{u}}} \tag{16}$$

$$\tilde{c} \ddot{\tilde{T}} + \tilde{\gamma} T_0 \,\mathrm{div}\, \ddot{\tilde{\mathbf{u}}} = \tilde{k}^* \nabla^2 \tilde{T} \tag{17}$$

where

$$\tilde{\gamma} = \left(3\tilde{\lambda} + 2\tilde{\mu} \right) \tilde{\beta}^* \tag{18}$$

The non-dimensional parameters considering randomness are

$$\bar{r} = \frac{r}{l}, \bar{t} = \frac{v}{l} t, \bar{\tilde{\mathbf{u}}} = \frac{1}{l} \frac{\left(\tilde{\lambda} + 2\tilde{\mu} \right)}{\tilde{\gamma} T_0} \tilde{\mathbf{u}}, \bar{\tilde{T}} = \frac{\tilde{T}}{T_0}, \bar{\tilde{\sigma}}_r = \frac{\tilde{\sigma}_r}{\tilde{\gamma} T_0}, \bar{\tilde{\sigma}}_\theta = \frac{\tilde{\sigma}_\theta}{\tilde{\gamma} T_0} \tag{19}$$

For the sake of brevity, the following terms are used

$$\hat{r} = \bar{\tilde{u}}, \quad \hat{T} = \bar{\tilde{T}}, \quad \hat{\sigma}_r = \overline{\hat{\sigma}_r}, \quad \hat{\sigma}_\theta = \overline{\hat{\sigma}_\theta} \tag{20}$$

The coupled themoelasticity governing equations with uncertainty in mechanical properties for axisymmetry and plane strain conditions can be obtained as follows

$$\tilde{C}_p^2 \frac{\partial^2 \hat{u}_r}{\partial \bar{r}^2} + \tilde{C}_p^2 \frac{1}{\bar{r}} \frac{\partial \hat{u}_r}{\partial \bar{r}} - (\tilde{C}_p^2 - \tilde{C}_s^2) \frac{\hat{u}_r}{\bar{r}^2} - \tilde{C}_p^2 \frac{\partial \hat{T}}{\partial \bar{r}} = \ddot{\hat{u}}_r \tag{21}$$

$$\tilde{C}_T^2 \left[\frac{\partial^2 \hat{T}}{\partial \bar{r}^2} + \frac{1}{\bar{r}} \frac{\partial \hat{T}}{\partial \bar{r}} \right] = \ddot{\hat{T}} + \hat{\varepsilon}^* \left[\frac{\partial \ddot{\hat{u}}_r}{\partial \bar{r}} + \frac{\ddot{\hat{u}}_r}{\bar{r}} \right] \tag{22}$$

For the sake of brevity, it is assumed that $\hat{u}_r = \hat{u}, \ddot{\hat{u}}_r = \ddot{\hat{u}}$. To solve the derived coupled

thermoelasticity equations with uncertainty in mechanical properties (21) and (22), some numerical methods requiring mesh generation or mesh reduction or meshless techniques can be employed. In this article, we explore the use of a very efficient method, called stochastic generalized finite difference (SGFD) method which is not requiring any mesh. In the SGFD method, the Monte Carlo simulation is used for random fields.

3. Solution technique

3.1 Stochastic generalized finite difference (SGFD) method

Here is developed the application of SGFD method without requiring any mesh generation for coupled thermoelasticity analysis based on Green -Naghdi theory for thick hollow cylinder. In this method, the partial derivatives are linearly approximated by Taylor series expansion on some nodes (center nodes) in the analyzed domain that each center node is surrounded by some other nodes. The partial derivatives of Taylor series expansion are obtained at the rest of each center nodes and the group of nodes with a center node and surrounding other nodes is called a star in this method.

Consider the non-dimensional radial displacement at a center node to be $\hat{u}_0$ and non-dimensional temperature to be $\hat{T}_0$ and the terms $\hat{u}_i$ and $\hat{T}_i$ are the values of non-dimensional radial displacement and temperature at the rest of surrounding nodes in each star. The function values $\hat{u}_i$ and $\hat{T}_i$ can be approximated using Taylor expansion as

$$\hat{u}_i = \hat{u}_0 + h_i \frac{\partial \hat{u}_0}{\partial \bar{r}} + \frac{1}{2}\left(h_i^2 \frac{\partial^2 \hat{u}_0}{\partial \bar{r}^2} \right) + \ldots \tag{23}$$

and

$$\hat{T}_i = \hat{T}_0 + h_i \frac{\partial \hat{T}_0}{\partial \bar{r}} + \frac{1}{2}\left(h_i^2 \frac{\partial^2 \hat{T}_0}{\partial \bar{r}^2} \right) + \ldots \tag{24}$$

The term i is number of surrounding nodes. The term h_i can be calculated as

$$h_i = \bar{r}_i - \bar{r}_o \tag{25}$$

The terms over second order are ignored in Eqs. (23) and (24) and the linear approximation of second order can be obtained for radial displacement and temperature. To minimize the error in this method, the function of norm should be minimized. The functions of norm for radial displacement and temperature are

$$\text{Norm}(\hat{u}) = \sum_{i=1}^{N} \left[\left(\hat{u}_0 - \hat{u}_i + h_i \frac{\partial \hat{u}_0}{\partial \bar{r}} + \frac{1}{2}\left(h_i^2 \frac{\partial^2 \hat{u}_0}{\partial \bar{r}^2} \right) \right) w(h_i) \right]^2 \tag{26}$$

and

$$\text{Norm}(\hat{T}) = \sum_{i=1}^{N}\left[\left(\hat{T}_0 - \hat{T}_i + h_i \frac{\partial \hat{T}_0}{\partial \bar{r}} + \frac{1}{2}\left(h_i^2 \frac{\partial^2 \hat{T}_0}{\partial \bar{r}^2}\right)\right) w(h_i)\right]^2 \tag{27}$$

where $w(h_i)$ is the weight function. In this article, we assume that the weight functions is defined by

$$w(h_i) = \frac{1}{(dist)^3} = \frac{1}{h_i^3} \tag{28}$$

If the norms (26) and (27) are minimized with respect to the partial derivatives, a set of linear equations system is obtained as follows

$$\psi^u{}_2 Q_{u2} = \xi^u{}_2 \tag{29}$$

$$\psi^T{}_2 Q_{T2} = \xi^T{}_2 \tag{30}$$

where the terms $\psi^u{}_2$ and $\psi^T{}_2$ stand for 2×2 matrices in displacement and temperature fields, respectively. The components of matrices $\psi^u{}_2$ and $\psi^T{}_2$ and vectors $\xi^u{}_2$ and $\xi^T{}_2$ are obtained in the Appendix. The vectors Q_{u2} and Q_{T2} are given, respectively, by

$$Q_{u2} = \left\{\frac{\partial \bar{u}_0}{\partial \bar{r}}, \frac{\partial^2 \bar{u}_0}{\partial \bar{r}^2}\right\}^T \tag{31}$$

$$Q_{T2} = \left\{\frac{\partial \bar{T}_0}{\partial \bar{r}}, \frac{\partial^2 \bar{T}_0}{\partial \bar{r}^2}\right\}^T \tag{32}$$

There are some methods to solve the system of differential equations that one of them is Cholesky method (Benito *et al*. 2007). In Cholesky method, the symmetric matrices $\psi^u{}_2$ and $\psi^T{}_2$ are decomposed to upper and lower triangular matrices. The method is explained as follows for $\psi^u{}_2$.

$$\psi^u{}_2 = L_2 L_2{}^T \tag{33}$$

The components of the matric L_2 are denoted by $l(i, j)$ with i, j=1, 2, …, P, where P=2 in our case, and

$$Q_{u2}(k) = \frac{1}{l(k,k)}\left(Y(k) - \sum_{i=1}^{P-k} l(k+i,k) Q_{u2}(k+i)\right) \quad (k = 1,...,P) \tag{34}$$

$$Y(k)=\left(-\bar{u}_0\sum_{i=1}^{P}M(k,i)c_i+\sum_{j=1}^{N}\bar{u}_j\left(\sum_{i=1}^{P}M(k,i)d_{ji}\right)\right)\ (k=1,...,P) \tag{35}$$

$$M(i,j)=(-1)^{i+j}\frac{1}{l(i,j)}\sum_{k=j}^{i-1}l(i,j)M(k,j)\ \ with\ \ j\prec i\ \ (i,j=1,...,P) \tag{36}$$

$$M(i,j)=\frac{1}{l(i,j)}\ \ with\ j=i\,(i,j=1,...,P) \tag{37}$$

$$M(i,j)=0\quad with\ \ j\succ i\,(i,j=1,...,P) \tag{38}$$

where

$$c_i=\sum_{j=1}^{N}d_{ji}\ ,\ d_{j1}=h_jW^2\ ,\ d_{j2}=\frac{h_j^{\,2}}{2}W^2 \tag{39}$$

and

$$W^2=\left(w(h_i)\right)^2 \tag{40}$$

The similar approach can be used for Q_{T2}. Also, the first and second derivatives can be calculated as

$$\frac{\partial\hat{u}_0}{\partial\bar{r}}=A_1^u\left\{\sum_{i=1}^{N}\left(-\hat{u}_0+\hat{u}_i\right)h_iw^2\left(h_i\right)\right\}-A_2^u\left\{\sum_{i=1}^{N}\left(-\hat{u}_0+\hat{u}_i\right)\frac{h_i^2}{2}w^2\left(h_i\right)\right\} \tag{41}$$

$$\frac{\partial^2\hat{u}_0}{\partial\bar{r}^2}=B_1^u\left\{\sum_{i=1}^{N}\left(-\hat{u}_0+\hat{u}_i\right)h_iw^2\left(h_i\right)\right\}-B_2^u\left\{\sum_{i=1}^{N}\left(-\hat{u}_0+\hat{u}_i\right)\frac{h_i^2}{2}w^2\left(h_i\right)\right\} \tag{42}$$

and

$$\frac{\partial\hat{T}_0}{\partial\bar{r}}=A_1^T\left\{\sum_{i=1}^{N}\left(-\hat{T}_0+\hat{T}_i\right)h_iw^2\left(h_i\right)\right\}-A_2^T\left\{\sum_{i=1}^{N}\left(-\hat{T}_0+\hat{T}_i\right)\frac{h_i^2}{2}w^2\left(h_i\right)\right\} \tag{43}$$

$$\frac{\partial^2\hat{T}_0}{\partial\bar{r}^2}=B_1^T\left\{\sum_{i=1}^{N}\left(-\hat{T}_0+\hat{T}_i\right)h_iw^2\left(h_i\right)\right\}-B_2^T\left\{\sum_{i=1}^{N}\left(-\hat{T}_0+\hat{T}_i\right)\frac{h_i^2}{2}w^2\left(h_i\right)\right\} \tag{44}$$

where the coefficients $A_1^u, A_2^u, B_1^u, B_2^u, A_1^T, A_2^T, B_1^T, B_2^T$ are obtained in details in Appendix. The derivatives of radial displacement and temperature can be also rewritten in star forms as follows

$$\frac{\partial\hat{u}_0}{\partial\bar{r}}=-\alpha_0\hat{u}_0+\sum_{i=1}^{N}\alpha_i\hat{u}_i \tag{45}$$

where

$$\alpha_0 = A_1{}^u \sum_{i=1}^{N} h_i{}^2 \, w^2\left(h_i\right) - A_2{}^u \sum_{i=1}^{N} \frac{h_i{}^2}{2} w^2\left(h_i\right) \tag{46}$$

$$\alpha_i = A_1{}^u \, h_i{}^2 \, w^2\left(h_i\right) - A_2{}^u \, \frac{h_i{}^2}{2} w^2\left(h_i\right) \tag{47}$$

$$\alpha_0 = \sum_{i=1}^{N} \alpha_i \tag{48}$$

For second derivative of radial displacement, we have

$$\frac{\partial^2 \hat{u}_0}{\partial \bar{r}^2} = -\beta_0 \hat{u}_0 + \sum_{i=1}^{N} \beta_i \hat{u}_i \tag{49}$$

where

$$\beta_0 = B_1{}^u \sum_{i=1}^{N} h_i{}^2 \, w^2\left(h_i\right) - B_2{}^u \sum_{i=1}^{N} \frac{h_i{}^2}{2} w^2\left(h_i\right) \tag{50}$$

$$\beta_i = B_1{}^u \, h_i{}^2 \, w^2\left(h_i\right) - B_2{}^u \, \frac{h_i{}^2}{2} w^2\left(h_i\right) \tag{51}$$

$$\beta_0 = \sum_{i=1}^{N} \beta_i \tag{52}$$

The temperature derivatives can be obtained using the similar method.

$$\frac{\partial \hat{T}_0}{\partial \bar{r}} = -\gamma_0 \hat{T}_0 + \sum_{i=1}^{N} \gamma_i \hat{T}_i \tag{53}$$

where

$$\gamma_0 = A_1{}^T \sum_{i=1}^{N} h_i{}^2 \, w^2\left(h_i\right) - A_2{}^T \sum_{i=1}^{N} \frac{h_i{}^2}{2} w^2\left(h_i\right) \tag{54}$$

$$\gamma_i = A_1{}^T \, h_i{}^2 \, w^2\left(h_i\right) - A_2{}^T \, \frac{h_i{}^2}{2} w^2\left(h_i\right) \tag{55}$$

$$\gamma_0 = \sum_{i=1}^{N} \gamma_i \tag{56}$$

For second derivative of temperature, it can be written as

$$\frac{\partial^2 \hat{T}_0}{\partial \bar{r}^2} = -\psi_0 \hat{T}_0 + \sum_{i=1}^{N} \psi_i \hat{T}_i \tag{57}$$

where

$$\psi_0 = B_1^T \sum_{i=1}^{N} h_i^2 \, w^2(h_i) - B_2^T \sum_{i=1}^{N} \frac{h_i^2}{2} w^2(h_i) \tag{58}$$

$$\psi_i = B_1^T \, h_i^2 \, w^2(h_i) - B_2^T \, \frac{h_i^2}{2} w^2(h_i) \tag{59}$$

$$\psi_0 = \sum_{i=1}^{N} \psi_i \tag{60}$$

Also, the second derivative of radial displacement with respect to time can be approximated for first derivative with respect to radius as follows

$$\frac{\partial \ddot{\hat{u}}_0}{\partial \bar{r}} = -\alpha_0 \ddot{\hat{u}}_0 + \sum_{i=1}^{N} \alpha_i \ddot{\hat{u}}_i \tag{61}$$

where the terms α_0 and α_i were introduced in Eq. (47). By substituting the obtained relations in star forms for first and second derivatives in governing Eqs. (21) and (22) at a center node, the coupled thermoelasticity governing equations can be obtained in new form based on SGFD method. In other words, the governing equations should be valid at every center node on analyzed domain.

$$\tilde{C}_p^2 \frac{\partial^2 \hat{u}_0}{\partial \bar{r}^2} + \tilde{C}_p^2 \frac{1}{\bar{r}_0} \frac{\partial \hat{u}_0}{\partial \bar{r}} - (\tilde{C}_p^2 - \tilde{C}_s^2) \frac{\hat{u}_0}{\bar{r}_0^2} - \tilde{C}_p^2 \frac{\partial \hat{T}_0}{\partial \bar{r}} = \ddot{\hat{u}}_0 \tag{62}$$

$$\tilde{C}_p^2 \left(-\beta_0 \hat{u}_0 + \sum_{i=1}^{N} \beta_i \hat{u}_i \right) + \tilde{C}_p^2 \frac{1}{\bar{r}_0} \left(-\alpha_0 \hat{u}_0 + \sum_{i=1}^{N} \alpha_i \hat{u}_i \right)$$

$$-\left(\tilde{C}_p^2 - \tilde{C}_s^2\right) \frac{\hat{u}_0}{\bar{r}_0^2} - \tilde{C}_p^2 \left(-\gamma_0 \hat{u}_0 + \sum_{i=1}^{N} \gamma_i \hat{u}_i \right) = \ddot{\hat{u}}_0 \tag{63}$$

$$\left\{ -\beta_0 \tilde{C}_p^2 - \alpha_0 \tilde{C}_p^2 \frac{1}{\bar{r}_0} - \left(\tilde{C}_p^2 - \tilde{C}_s^2\right) \frac{1}{\bar{r}_0^2} \right\} \hat{u}_0 + \sum_{i=1}^{N} \left\{ \tilde{C}_p^2 \beta_i + \tilde{C}_p^2 \frac{1}{\bar{r}_0} \alpha_i \right\} \hat{u}_i$$

$$+\left\{\tilde{C}_p^2\gamma_0\right\}\hat{T}_0+\sum_{i=1}^{N}\left\{-\tilde{C}_p^2\gamma_i\right\}\hat{T}_i=\ddot{\hat{u}}_0 \tag{64}$$

and also the second governing equation can be written as

$$\tilde{C}_T^2\left[\frac{\partial^2\hat{T}_0}{\partial\bar{r}^2}+\frac{1}{\bar{r}_0}\frac{\partial\hat{T}_0}{\partial\bar{r}}\right]=\ddot{\hat{T}}_0+\varepsilon^*\left[\frac{\partial\ddot{\hat{u}}_0}{\partial\bar{r}}+\frac{\ddot{\hat{u}}_0}{\bar{r}_0}\right] \tag{65}$$

The following system of equations is obtained for the distributed nodes on the analyzed domain.

$$\left[M\right]_{(N+1)*(N+1)}\left\{\ddot{\phi}\right\}_{(N+1)*1}+\left[K\right]_{(N+1)*(N+1)}\left\{\phi\right\}_{(N+1)*1}=\left[f\right]_{(N+1)*1} \tag{68}$$

where

$$\left\{\phi\right\}^T=\left\{\hat{u}_0\quad\hat{T}_0\quad\hat{u}_1\quad\hat{T}_1\quad\ldots\quad\hat{u}_N\quad\hat{T}_N\right\}^T \tag{69}$$

and

$$\left\{\ddot{\phi}\right\}^T=\left\{\ddot{\hat{u}}_0\quad\ddot{\hat{T}}_0\quad\ddot{\hat{u}}_1\quad\ddot{\hat{T}}_1\quad\ldots\quad\ddot{\hat{u}}_N\quad\ddot{\hat{T}}_N\right\}^T \tag{70}$$

3.2 Time domain analysis stochastic

There are some numerical methods to solve the system of equations based on SGFD method (68). In this article, the Newmark finite difference method with suitable time step is used and the dynamic behavior of temperature and displacement domains are obtained for the cylinder.

Consider the system to be in non-dimensional time $\bar{t}=t_p$ in which the governing equation of system is shown as follows

$$\left[M\right]\left\{\ddot{\phi}^{t_p}\right\}+\left[K\right]\left\{\phi^{t_p}\right\}=\left[f^{t_p}\right] \tag{71}$$

Using the initial conditions $\{f^0\}$ and $\{\phi^0\}$, the following equation can be concluded as

$$\left[M\right]\left\{\ddot{\phi}^0\right\}=\left\{f^0\right\}-\left[K\right]\left\{\phi^0\right\} \tag{72}$$

The new matrices can be defined as follows

$$\left[K_m\right]=\left[K\right]+\frac{1}{\lambda_1\Delta t^2}\left[M\right] \tag{73}$$

$$\left\{f_m^{t_p}\right\}=\left\{f^{t_p}\right\}+\frac{1}{\lambda_1\Delta t^2}\left[M\right]\left(\left\{\phi^{t_p-1}\right\}+\Delta t\left\{\dot{\phi}^{t_p-1}\right\}+\left(0.5-\lambda_1\right)\Delta t^2\left\{\ddot{\phi}^{t_p-1}\right\}\right) \tag{74}$$

The matrices of $\left\lfloor\phi^{t_p}\right\rfloor$, $\left\lfloor\dot{\phi}^{t_p}\right\rfloor$ and $\left\lfloor\ddot{\phi}^{t_p}\right\rfloor$ can be calculated using following equations.

$$\left\{\phi^{t_p}\right\}=\left[K_m\right]^{-1}\left\{f_m^{t_p}\right\} \tag{75}$$

$$\left\{\ddot{\phi}^{t_p}\right\}=\frac{1}{\lambda_1\Delta t^2}\left(\left\{\phi^{t_p}\right\}-\left\{\phi^{t_p-1}\right\}-\Delta t\left\{\dot{\phi}^{t_p-1}\right\}-\Delta t^2\left(0.5-\lambda_1\right)\left\{\ddot{\phi}^{t_p-1}\right\}\right) \tag{76}$$

$$\left\{\dot{\phi}^{t_p}\right\}=\left\{\dot{\phi}^{t_p-1}\right\}+\Delta t\left[\left(1-\lambda_2\right)\left\{\ddot{\phi}^{t_p-1}\right\}+\lambda_2\left\{\ddot{\phi}^{t_p}\right\}\right] \tag{77}$$

Using aforementioned equations, the matrices of $\{f^0\}$ and $\{\phi^0\}$can be obtained for an arbitrary time. The best convergence rate can be reached in this method by choosing λ_1=1/4 and λ_2=1/2.

4. Numerical examples and discussions

To study the thermoelastic wave propagation in thick hollow cylinder, we consider an axisymmetric hollow cylinder in plane strain conditions with inner and outer radii $\bar{r}_{in}$ and $\bar{r}_{out}$, respectively, which was defined in previous section. The term H is defined as $H=\bar{r}_{out}-\bar{r}_{in}$ and $H(\bar{t})$ stands for Heaviside unit step function.

The mechanical properties are generated as random variables, with mean value equal to the deterministic value of mechanical properties presented (Taheri *et al*. 2005) as follows

$$C_p=0.5,\quad C_T=1.0,\quad C_s=0.267,\quad \varepsilon^*=0.073 \tag{78}$$

The random variables are generated with Gaussian distribution (Normal distribution) having various coefficients of variations (COVs) such as COV=2.5%, COV=5% and COV=10%. To verify the results and method of solution, the mean values of results in both non-dimensional radial displacement and temperature are compared to the presented results based on the locally transversal linearization (LTL) method (Teheri *et al*. 2005) and also with presented data based on meshless local Petrov-Galerkin (MLPG) method (Hosseini *et al*. 2011c). The inner surface of cylinder is assumed to be under suddenly heat flux, the outer surface is isolated and radial displacement of nodes on both inner and outer surfaces are considered to be fixed.

$$\dot{q}\left(\bar{r}_{in},\bar{t}\right)=-H\left(\bar{t}\right),\quad \bar{u}\left(\bar{r}_{in},\bar{t}\right)=0 \tag{79}$$

$$\frac{\partial\bar{T}\left(\bar{r}_{out},\bar{t}\right)}{\partial\bar{r}}=0\ ,\quad \bar{u}\left(\bar{r}_{out},\bar{t}\right)=0 \tag{80}$$

where $\dot{q}$ is the heat flux that is defined in the GN theory of coupled thermoelasticity as

$$\dot{q}\left(\bar{r},\bar{t}\right)=-C_T{}^2\frac{\partial\bar{T}\left(\bar{r},\bar{t}\right)}{\partial\bar{r}} \tag{81}$$

In GFD method, we consider N nodes distributed on thickness of cylinder through radial

direction and the first node i=1 is located on inner surface and the last one i=N is located on outer surface of cylinder.

The non-dimensional temperature distributions through radial direction of cylinder are depicted at various non-dimensional time using three different methods including SGFD (presented method), MLPG and LTL methods. The comparison between results of these three methods shows that the SGFD method is an effective method with high capability for coupled thermoelasticity analysis considering uncertainty in some inputs parameters. Also, the propagation of thermal wave through radial direction of cylinder (across thickness) can be seen in Fig. 1 at various non-dimensional times. The similar behavior can be found for non-dimensional radial displacement distribution, which is illustrated in Fig. 2. The propagation of non-dimensional radial displacement distributions based on three numerical methods are plotted in Fig. 2 for comparison. It can be also concluded from Fig. 2 that the obtained results (mean values) from SGFD method are in good agreement with the MLPG and LTL results at different non-dimensional times. The non-dimensional radial displacement wave front can be tracked in Fig. 2.

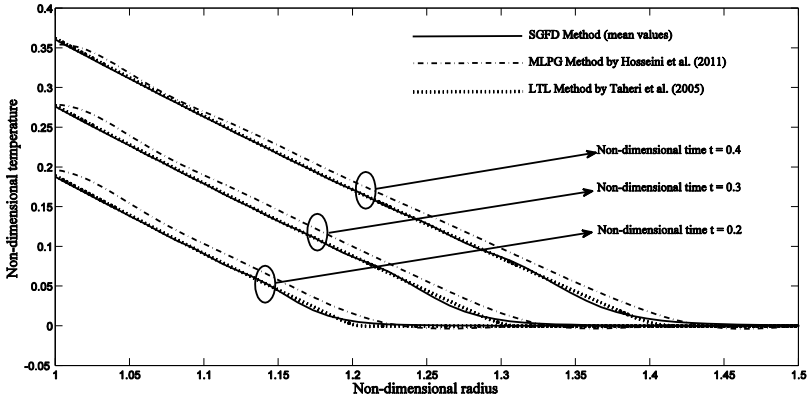

Fig. 1 Thermal wave propagation through radial direction across thickness of cylinder in first example

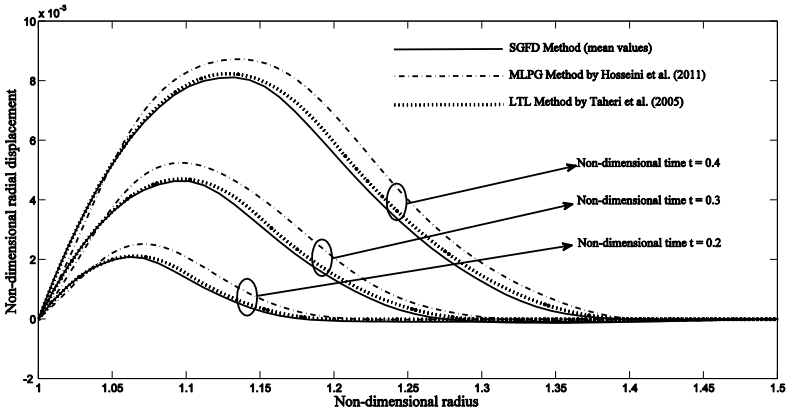

Fig. 2 Radial displacement wave propagation through radial direction across thickness of cylinder in first example

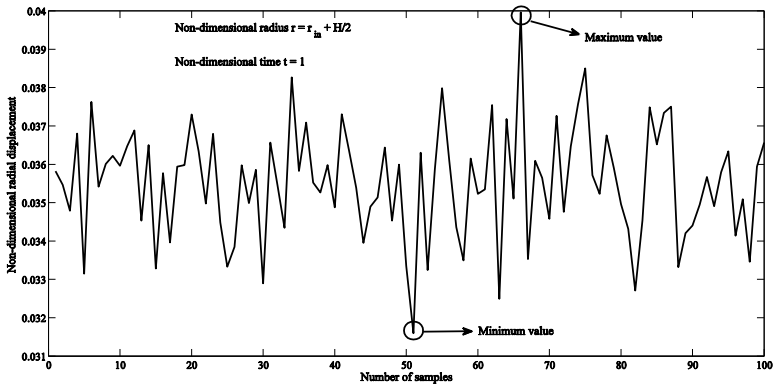

Fig. 3 Variation of non-dimensional radial displacement versus number of samples in Monte Carlo simulations

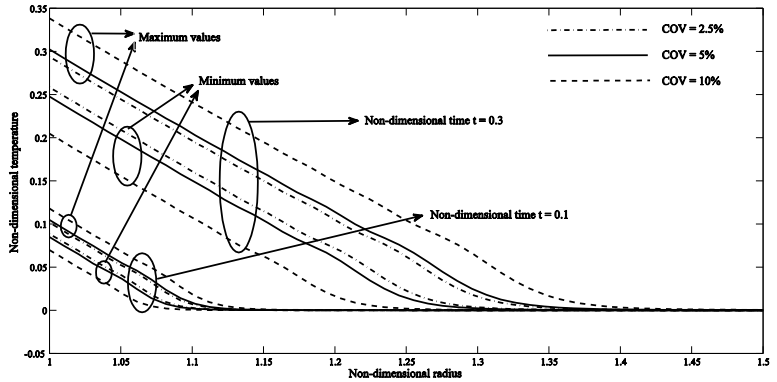

Fig. 4 Maximum and minimum values of non-dimensional temperature distributions across thickness of cylinder for various values of COV and non-dimensional times at first example

The results in time and displacement domains are random variables, if the inputs such as mechanical properties of cylinder are considered as random parameters and generated by Monte Carlo simulations. Consequently, for certain time and radius, the results can be found as random values, which are distributed around a mean values. Fig. 3 shows the random results versus number of samples in Monte Carlo simulation for radial displacement domain at $\bar{t}=1$ for middle point of thickness. The maximum and minimum values are shown in this figure. The propagations of thermal wave based on maximum and minimum values of temperature are drawn in Fig. 4 for $\bar{t}=0.1 \text{and} \bar{t}=0.3$. The difference between minimum and maximum values is increased by increasing of coefficient of variations (COVs), which can be concluded from Fig. 4. From engineering perspective, it means that the maximum or minimum values of non-dimensional temperature should be considered for designing purposes. Also, the estimation of thermal wave speed is different based on minimum and maximum values of non-dimensional temperature. It can be seen in Fig. 4 that the wave front for maximum values is propagated faster than minimum values. The similar behavior can be seen for non-dimensional radial displacement distribution,

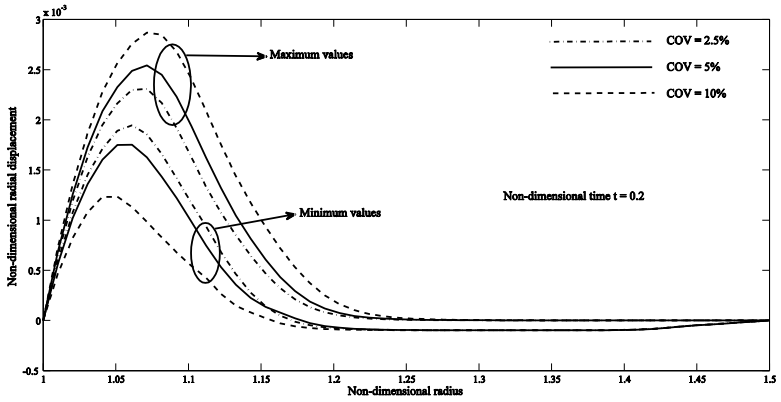

Fig. 5 Maximum and minimum values of non-dimensional radial displacement distributions across thickness of cylinder for various values of COV at a certain non-dimensional time in first example

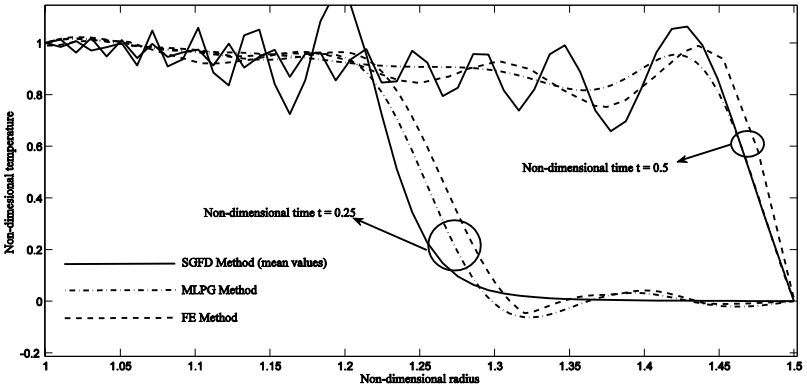

Fig. 6 Thermal wave propagation along radial direction in second example

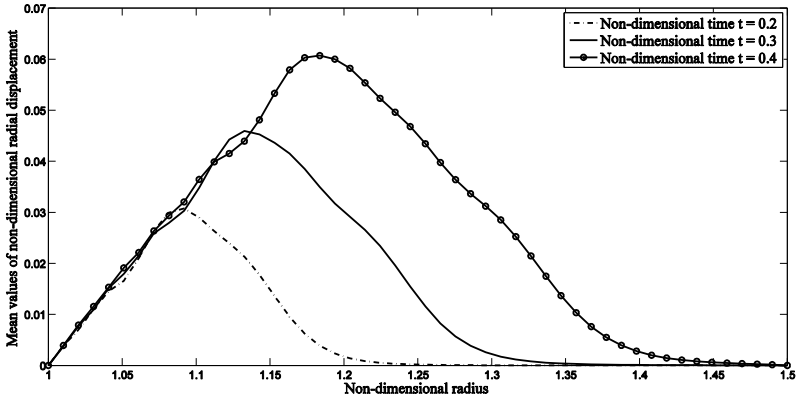

Fig. 7 Radial displacement wave propagation based on mean values along radial direction of cylinder in second example

which is shown in Fig. 5 for $\bar{t} = 0.2$ and various values of COV. Also, the wave front of maximum non-dimensional radial displacement s is propagated faster than minimum values for each value of COV.

To show more abilities of GFD method in coupled thermoelasticity case, the following thermal shock loading is considered as second example. The inner surface of cylinder is assumed to be under suddenly temperature rising and simply supported conditions for displacements as follows

$$\bar{T}\left(\bar{r}_{in}, \bar{t}\right) = H\left(\bar{t}\right), \quad \bar{u}\left(\bar{r}_{in}, \bar{t}\right) = 0 \tag{82}$$

$$\bar{T}\left(\bar{r}_{out}, \bar{t}\right) = 0 \ , \quad \bar{u}\left(\bar{r}_{out}, \bar{t}\right) = 0 \tag{83}$$

where $H(\bar{t})$ is the Heaviside unit step function. In the GFD method, there is no any interpolation or discretization on boundary conditions. It can be considered as another advantage of the SGFD method.

The propagation of thermal wave has been obtained through radial direction across thickness of cylinder using three numerical methods including finite element (FE), MLPG and SGFD methods, which the results are drawn in Fig. 6. Also, the Fig. 6 shows us the obtained results using SGFD method have a good agreement with those obtained using other methods in second example too. There are some fluctuations before thermal wave front in the diagrams of results. The main justification of this physical phenomenon is the disturbances in displacement and temperature fields, which are created by shock loading. The fluctuations depend on the selected parameters of GN theory such as C_p, C_T and C_s and also depend on the some parameters of solution methods. The non-dimensional radial displacement wave propagation based on mean values can be tracked in radial direction on thickness of cylinder at various times, which can be found in Fig. 7. The time history of non-dimensional radial displacement and temperature based on mean values at various point on thickness are shown in Fig. 8 and Fig. 9, respectively.

In Fig. 9, the non-dimensional temperature of point close to inner surface $\bar{r} = \bar{r}_{in} + H/4$ starts to oscillate earlier than other points. It means that the thermal wave front reaches to this point earlier than other point, which is compatible with realistic behavior of temperature domain from physical view. Both dynamic behaviors of non-dimensional radial displacement and temperature in time domain show a periodic behavior. There is no any damping in these periodic waves that shows a good compatibility with GN theory of coupled thermoelasticity without energy dissipation. Also, these behaviors in time domain can be used to estimate the velocity of thermal and non-dimensional radial displacement waves propagation. The application of SGFD method in coupled thermoelasticity furnishes a ground to study the wave propagation analysis and also natural frequency analysis using time history of non-dimensional variables. The authors would like to develop the application of SGFD method to aforementioned analysis in their future works.

Fig. 10 shows the differences between maximum and minimum values distributions across thickness of cylinder for various values of COV. The differences are increased by increasing the values of COV. Also, it is concluded that the thermal wave fronts for maximum values are propagated faster than minimum values. The propagation of maximum values of non-dimensional temperatures are depicted in Fig. 11 for COV=5%. The time histories of maximum values, which are depicted for middle point of thickness and various values of COV in Fig. 12, show the similar behaviors. The differences between maximum values and results obtained from deterministic inputs are increased by increasing the value of COV. Fig. 13 is drawn to show the comparison of time histories of maximum values and time history of result obtained from deterministic inputs in

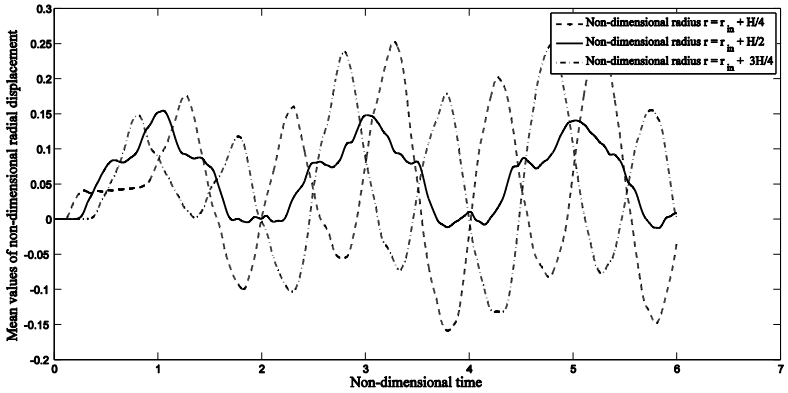

Fig. 8 Time history of non-dimensional radial displacement mean values at various points of thickness in second example

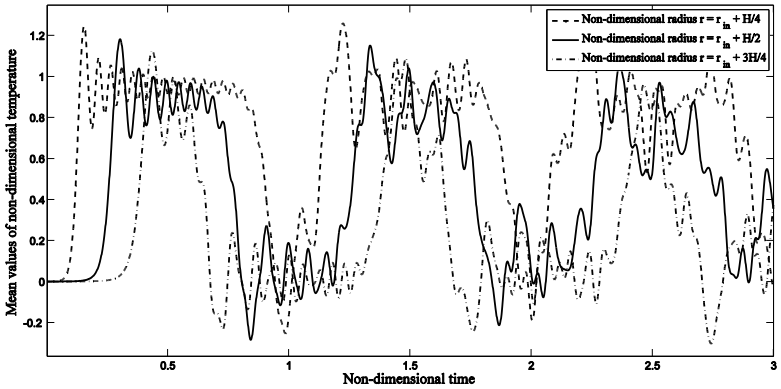

Fig. 9 Time history of non-dimensional temperature mean values at various points of thickness in second example

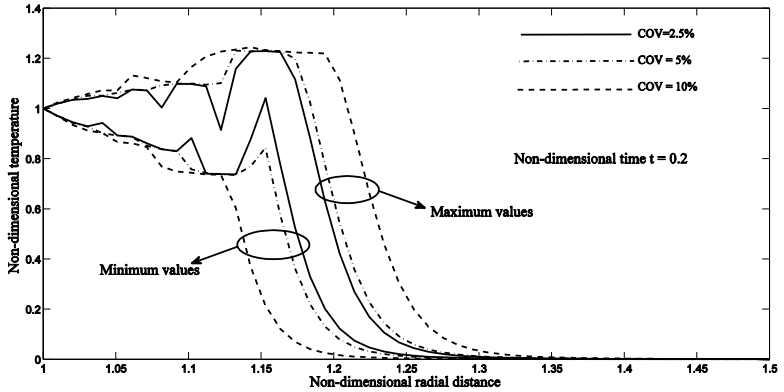

Fig. 10 The comparison of maximum and minimum values distributions across thickness of cylinder in non-dimensional temperature domain for various values of COV in second example

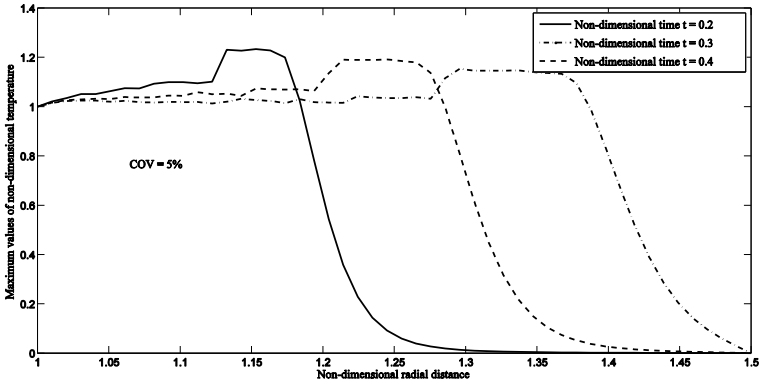

Fig. 11 The propagation of maximum non-dimensional temperature across thickness of cylinder for COV = 5% at various non-dimensional time in second example

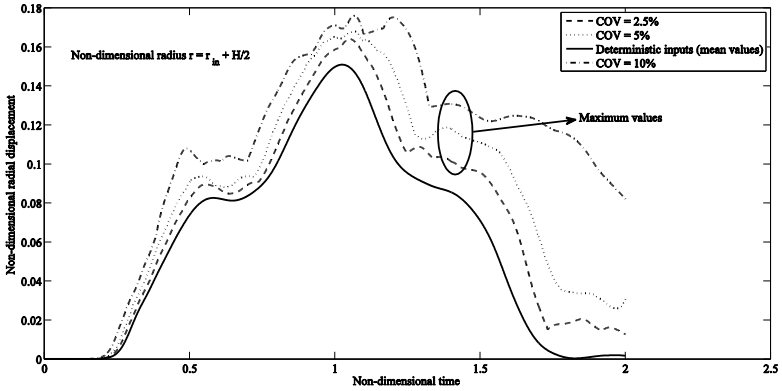

Fig. 12 The comparison between time histories of non-dimensional radial displacement maximum values and time history based on deterministic inputs in second example

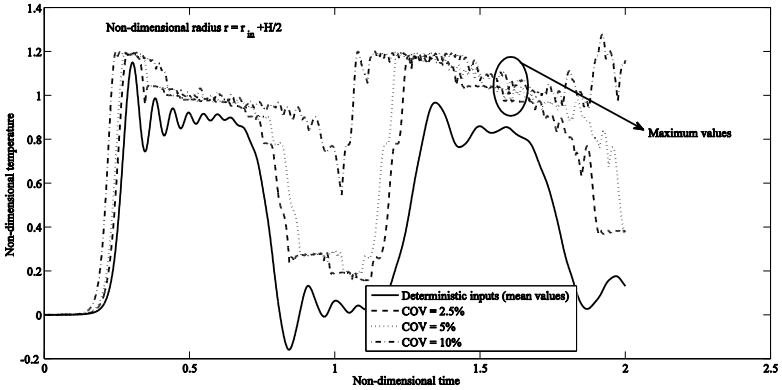

Fig. 13 The comparison between time histories of non-dimensional temperature maximum values and time history based on deterministic inputs in second example

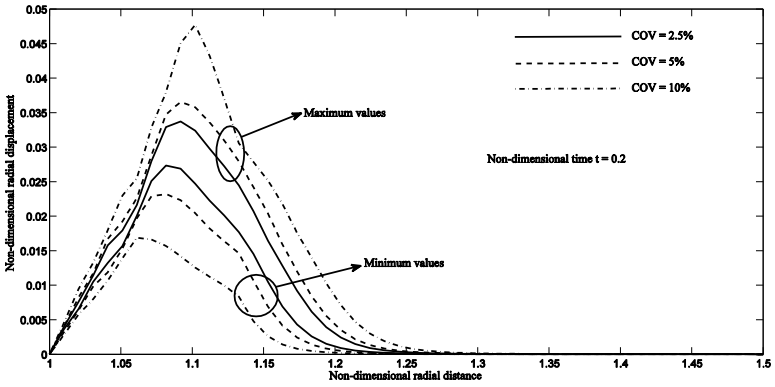

Fig. 14 The distribution of maximum and minimum values of non-dimensional radial displacement across thickness of cylinder for various COV in second example

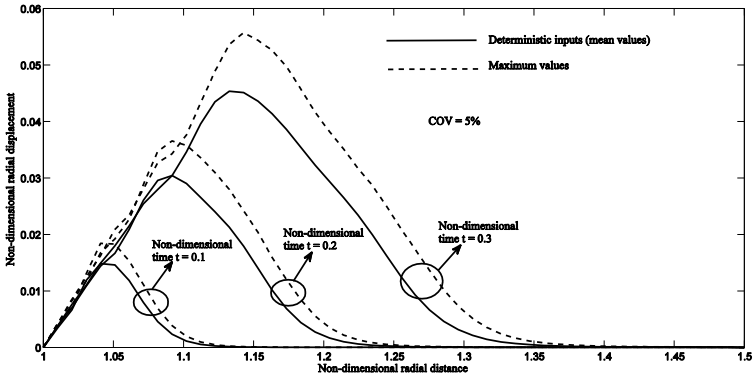

Fig. 15 The comparison between distribution of non-dimensional radial displacement maximum values for COV = 5% and time history based on deterministic inputs at various non-dimensional times in second example

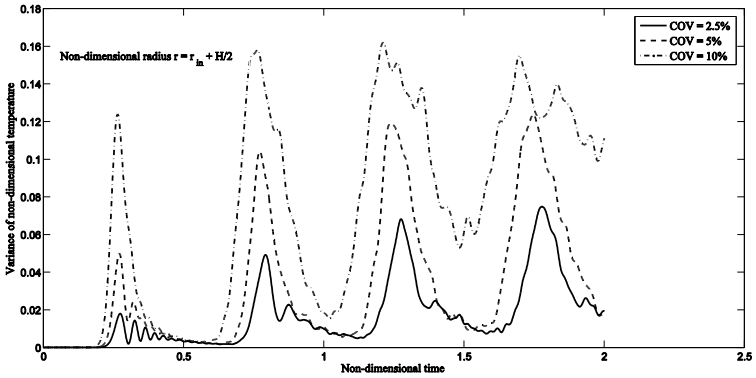

Fig. 16 Time histories of variance of non-dimensional temperature for middle point of thickness and various COV in second example

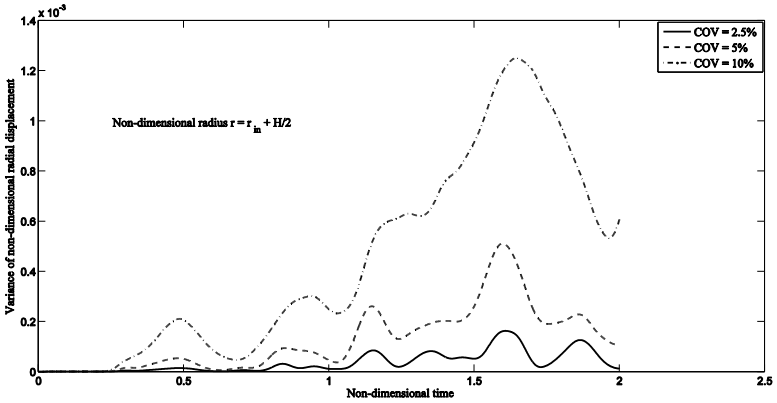

Fig. 17 Time histories of variance of non-dimensional radial displacement for middle point of thickness and various COV in second example

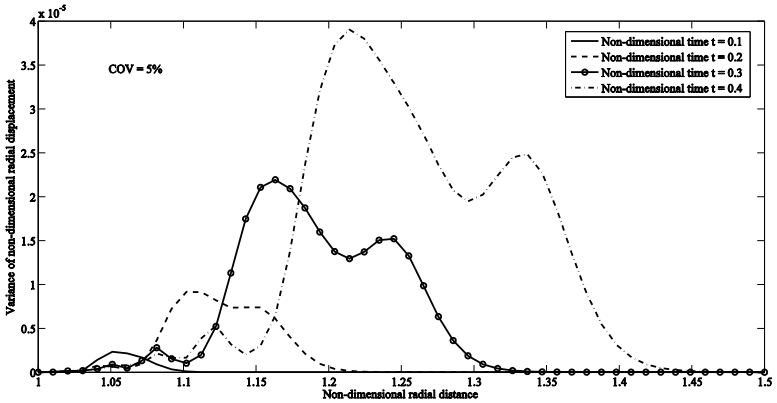

Fig. 18 The distributions of non-dimensional radial displacement across thickness of cylinder for COV = 5% at various non-dimensional times in second example

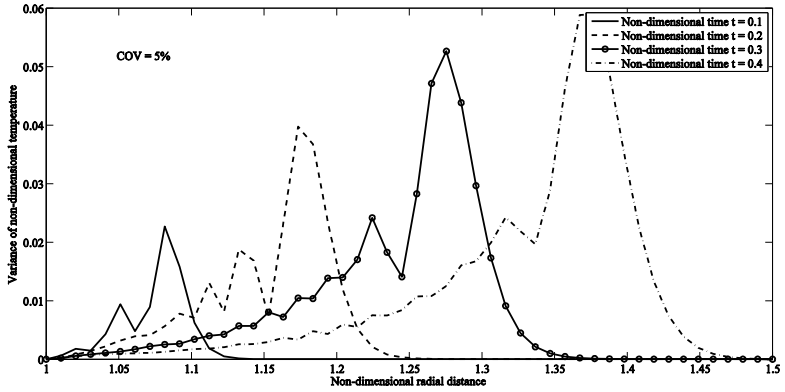

Fig. 19 he distributions of non-dimensional temperature across thickness of cylinder for COV = 5% at various non-dimensional times in second example

non-dimensional temperature domain. The non-dimensional radial displacement distributions across thickness of cylinder for minimum and maximum values can be compared together in Fig. 14 for various values of COV at $\bar{t} = 0.2$. Also, the elastic wave propagation based on maximum values and the obtained results from deterministic inputs can be found in Fig. 15 at various non-dimensional times and COV=5%.

Figs. 16 and 17 show the time histories of variance of non-dimensional temperature and radial displacement for middle point of thickness and various values of COV, respectively. The peak points in diagrams are increased by increasing the values of COV and the biggest one is for COV=10%. The distributions of variance across thickness of cylinder for non-dimensional radial displacement and temperature are illustrated in Figs. 18 and 19, respectively. In both figures, the distributions are plotted for COV=5% at various non-dimensional times. Also, the propagations of variances can be tracked through radial direction of cylinder.

5. Conclusions

The application of a stochastic hybrid mesh-free method based on stochastic generalized finite difference (SGFD) method has been developed to solve the coupled thermoelasticity governing equations based on Green-Naghdi theory (without energy dissipation) in media with Gaussian uncertainty in mechanical properties. The second sound phenomenon is stochastically studied in details. The thick hollow cylinder is considered as the analyzed domain for the problem, which is under thermal shock loading. The axi-symmetry and plane strain conditions are assumed in this article. The main outputs of this paper can be outlined as follows.

- The governing coupled thermoelasticity equations of thick hollow cylinder are derived in SGFD forms. The propagations of thermal and non-dimensional radial displacement waves through radial direction of cylinder are simulated and discussed in details for two kinds of thermal shock loading.
- The elastic wave propagation and second sound are stochastically studied in details. Also, the effects of COV on second sound are determined and discussed in both non-dimensional temperature and radial displacement domains.
- The uncertainty in mechanical properties influences on the thermal and elastic wave propagation through radial direction and also on the time histories in temperature and displacement domains. The thermal and elastic wave fronts are different for maximum and minimum values, which are discussed in details in the paper. Also, the value of COV influences on the distributions and time histories of temperature and displacement.
- The time history of non-dimensional temperature and radial displacement show periodic wave that furnishes a ground to use the SGFD method to estimate the wave propagation velocity with uncertainty in some parameters in teh problem and also for natural frequency analysis of cylinders. It is concluded from presented results in the paper that the thermal and elastic wave velocity are different for maximum and minimum values.

In general, the paper develops the application of the presented stochastic hybrid mesh-free method based on SGFD method in thermoelastic wave propagation and stochastic coupled thermoelasticity analysis of thick cylinder as an efficient method.

Acknowledgements

This work is supported by Ferdowsi University of Mashhad as a research project with No. 2/20600 and date (14-02-2012).

References

Bagri, A. and Eslami, M.R. (2007a), "A unified generalized thermoelasticity; solution for cylinders and spheres", *Int. J. Mech. Sci.*, **49**, 1325-1335.

Bagri, A. and Eslami, M.R. (2007b), "A unified generalized thermoelasticity formulation; application to thick functionally graded cylinders", *J. Thermal Stress.*, **30**, 911-930.

Benito, J.J., Urena, F. and Gavete, L. (2001), "Influence of several factors in the generalized finite difference method", *Appl. Math. Model.*, **25**(12), 1039-1053.

Benito, J.J., Urena, F. and Gavete, L. (2003), "An h-adaptive method in the generalized finite differences", *Comput. Meth. Appl. Mech. Eng.*, **192**, 735-739.

Benito, J.J., Urena, F. and Gavete, L. (2007), "Solving parabolic and hyperbolic equations by the generalized finite difference method", *J. Comput. Appl. Math.*, **209**, 208-233.

Chandrasekharaiah, D.S. (1998), "Hyperbolic thermoelasticity: a review of recent literature", *Appl. Mech. Rev.*, **51**, 705-729.

Chiba, R. and Sugano, Y. (2008), "Stochastic analysis of a thermoelastic problem in functionally graded plates with uncertain material properties", *Arch. Appl. Mech.*, **78**(10), 749-764.

Chiba, R. (2009), "Stochastic thermal stresses in an FGM annular disc of variable thickness with spatially random heat transfer coefficients", *Meccanica*, **44**(2), 159-176.

Gavete, L., Benito, J.J. and Gavete, M.L. (2003), "Improvements of generalized finite difference method and comparison with other meshless method", *Appl. Math. Model.*, **27**(10), 831-847.

Green, A. E. and Naghdi, P. M. (1993), "Thermoelasticity without energy dissipation", *J. Elastic.*, **31**, 189-208.

Hosseini, S.M., Akhlaghi, M. and Shakeri, M. (2008), "Heat conduction and heat wave propagation in functionally graded thick hollow cylinder base on coupled thermoelasticity without energy dissipation", *Heat Mass Tran.*, **44**, 1477-1484.

Hosseini, S.M. (2009), "Coupled thermoelasticity and second sound in finite length functionally graded thick Hollow cylinders (without energy dissipation)", *Mater. Des.*, **30**, 2011-2023.

Hosseini, S.M. and Shahabian, F. (2011a), "Transient analysis of thermo-elastic waves in thick Hollow cylinders using a stochastic hybrid numerical method, considering Gaussian mechanical properties", *Appl. Math. Model.*, **35**, 4697-4714.

Hosseini, S.M. and Shahabian, F. (2011b), "Stochastic assessment of thermo-elastic wave propagation in Functionally Graded Materials (FGMs) with Gaussian uncertainty in constitutive mechanical properties", *J. Thermal Stress.*, **34**, 1071-1099.

Hosseini, S.M., Sladek, J. and Sladek, V. (2011c), "Meshless local Petrov-Galerkin method for coupled thermo-elasticity analysis of a functionally graded thick Hollow cylinder", *Eng. Anal. Bound. Elem.*, **35**, 827-835.

Hosseini, S.M., Shahabian, F., Sladek, J. and Sladek, V. (2011d), "Stochastic meshless local Petrov-Galerkin (MLPG) method for thermo-elastic wave propagation analysis in functionally graded thick hollow cylinders", *Comput. Model. Eng. Sci.*, **71**(1), 39-66.

Melnik, R.V.N. (2001), "Discrete models of coupled dynamic thermoelasticity for stress-temperature formulations", *Appl. Math. Comput.*, **122**, 107-1328.

Sherief, H.H., El-Maghraby, N.M. and Allam, A. (2013), "Stochastic thermal shock problem in generalized thermoelasticity", *Appl. Math. Model.*, **37**(3), 762-775.

Taheri, H., Fariborz, S. and Eslami, M.R. (2005), "Thermoelastic analysis of an annulus using the Green-Naghdi model", *J. Thermal Stress.*, **28**(9), 911-927.

Appendix

The first and second derivations of non-dimensional radial displacement and temperatures can be calculated using following method.

$$\begin{bmatrix} \sum_{i=1}^{N} h_i^{\,2} w^2(h_i) & \sum_{i=1}^{N} \frac{h_i^{\,3}}{2} w^2(h_i) \\ \sum_{i=1}^{N} \frac{h_i^{\,3}}{2} w^2(h_i) & \sum_{i=1}^{N} \frac{h_i^{\,4}}{4} w^2(h_i) \end{bmatrix} \begin{Bmatrix} \frac{\partial \bar{u}_0}{\partial \bar{r}} \\ \frac{\partial^2 \bar{u}_0}{\partial \bar{r}^2} \end{Bmatrix} = \begin{bmatrix} \sum_{i=1}^{N} (-\bar{u}_0 + \bar{u}_i) h_i w^2(h_i) \\ \sum_{i=1}^{N} (-\bar{u}_0 + \bar{u}_i) \frac{h_i^{\,2}}{2} w^2(h_i) \end{bmatrix} \tag{A-1}$$

and

$$\begin{bmatrix} \sum_{i=1}^{N} h_i^{\,2} w^2(h_i) & \sum_{i=1}^{N} \frac{h_i^{\,3}}{2} w^2(h_i) \\ \sum_{i=1}^{N} \frac{h_i^{\,3}}{2} w^2(h_i) & \sum_{i=1}^{N} \frac{h_i^{\,4}}{4} w^2(h_i) \end{bmatrix} \begin{Bmatrix} \frac{\partial \bar{T}_0}{\partial \bar{r}} \\ \frac{\partial^2 \bar{T}_0}{\partial \bar{r}^2} \end{Bmatrix} = \begin{bmatrix} \sum_{i=1}^{N} (-\bar{T}_0 + \bar{T}_i) h_i w^2(h_i) \\ \sum_{i=1}^{N} (-\bar{T}_0 + \bar{T}_i) \frac{h_i^{\,2}}{2} w^2(h_i) \end{bmatrix} \tag{A-1}$$

The first and second derivatives are calculated as

$$\frac{\partial \bar{u}_0}{\partial \bar{r}} = A_1^{\,u} \left\{ \sum_{i=1}^{N} (-\bar{u}_0 + \bar{u}_i) h_i w^2(h_i) \right\} - A_2^{\,u} \left\{ \sum_{i=1}^{N} (-\bar{u}_0 + \bar{u}_i) \frac{h_i^{\,2}}{2} w^2(h_i) \right\} \tag{A-2}$$

$$\frac{\partial^2 \bar{u}_0}{\partial \bar{r}^2} = B_1^{\,u} \left\{ \sum_{i=1}^{N} (-\bar{u}_0 + \bar{u}_i) h_i w^2(h_i) \right\} - B_2^{\,u} \left\{ \sum_{i=1}^{N} (-\bar{u}_0 + \bar{u}_i) \frac{h_i^{\,2}}{2} w^2(h_i) \right\} \tag{A-3}$$

and

$$\frac{\partial \bar{T}_0}{\partial \bar{r}} = A_1^{\,T} \left\{ \sum_{i=1}^{N} (-\bar{T}_0 + \bar{T}_i) h_i w^2(h_i) \right\} - A_2^{\,T} \left\{ \sum_{i=1}^{N} (-\bar{T}_0 + \bar{T}_i) \frac{h_i^{\,2}}{2} w^2(h_i) \right\} \tag{A-4}$$

$$\frac{\partial^2 \bar{T}_0}{\partial \bar{r}^2} = B_1^{\,T} \left\{ \sum_{i=1}^{N} (-\bar{T}_0 + \bar{T}_i) h_i w^2(h_i) \right\} - B_2^{\,T} \left\{ \sum_{i=1}^{N} (-\bar{T}_0 + \bar{T}_i) \frac{h_i^{\,2}}{2} w^2(h_i) \right\} \tag{A-5}$$

where

$$A_1^{\,u} = \frac{\left(\sum_{i=1}^{N} \frac{h_i^{\,4}}{4} w^2(h_i) \right)}{\left(\sum_{i=1}^{N} h_i^{\,2} w^2(h_i) \right) \left(\sum_{i=1}^{N} \frac{h_i^{\,4}}{4} w^2(h_i) \right) - \left(\sum_{i=1}^{N} \frac{h_i^{\,3}}{2} w^2(h_i) \right)^2} \tag{A-6}$$

$$A_2^{\,u}=\frac{\left(\sum_{i=1}^{N}\frac{h_i^{\,3}}{2}w^2(h_i)\right)}{\left(\sum_{i=1}^{N}h_i^{\,2}\,w^2(h_i)\right)\left(\sum_{i=1}^{N}\frac{h_i^{\,4}}{4}w^2(h_i)\right)-\left(\sum_{i=1}^{N}\frac{h_i^{\,3}}{2}w^2(h_i)\right)^2} \tag{A-7}$$

$$B_1^{\,u}=\frac{-\left(\sum_{i=1}^{N}\frac{h_i^{\,3}}{2}w^2(h_i)\right)}{\left(\sum_{i=1}^{N}h_i^{\,2}\,w^2(h_i)\right)\left(\sum_{i=1}^{N}\frac{h_i^{\,4}}{4}w^2(h_i)\right)-\left(\sum_{i=1}^{N}\frac{h_i^{\,3}}{2}w^2(h_i)\right)^2} \tag{A-8}$$

$$B_2^{\,u}=\frac{-\left(\sum_{i=1}^{N}h_i^{\,2}\,w^2(h_i)\right)}{\left(\sum_{i=1}^{N}h_i^{\,2}\,w^2(h_i)\right)\left(\sum_{i=1}^{N}\frac{h_i^{\,4}}{4}w^2(h_i)\right)-\left(\sum_{i=1}^{N}\frac{h_i^{\,3}}{2}w^2(h_i)\right)^2} \tag{A-9}$$

and also

$$A_1^{\,T}=\frac{\left(\sum_{i=1}^{N}\frac{h_i^{\,4}}{4}w^2(h_i)\right)}{\left(\sum_{i=1}^{N}h_i^{\,2}\,w^2(h_i)\right)\left(\sum_{i=1}^{N}\frac{h_i^{\,4}}{4}w^2(h_i)\right)-\left(\sum_{i=1}^{N}\frac{h_i^{\,3}}{2}w^2(h_i)\right)^2} \tag{A-10}$$

$$A_2^{\,T}=\frac{\left(\sum_{i=1}^{N}\frac{h_i^{\,3}}{2}w^2(h_i)\right)}{\left(\sum_{i=1}^{N}h_i^{\,2}\,w^2(h_i)\right)\left(\sum_{i=1}^{N}\frac{h_i^{\,4}}{4}w^2(h_i)\right)-\left(\sum_{i=1}^{N}\frac{h_i^{\,3}}{2}w^2(h_i)\right)^2} \tag{A-11}$$

$$B_1^{\,T}=\frac{-\left(\sum_{i=1}^{N}\frac{h_i^{\,3}}{2}w^2(h_i)\right)}{\left(\sum_{i=1}^{N}h_i^{\,2}\,w^2(h_i)\right)\left(\sum_{i=1}^{N}\frac{h_i^{\,4}}{4}w^2(h_i)\right)-\left(\sum_{i=1}^{N}\frac{h_i^{\,3}}{2}w^2(h_i)\right)^2} \tag{A-12}$$

$$B_2^{\,T}=\frac{-\left(\sum_{i=1}^{N}h_i^{\,2}\,w^2(h_i)\right)}{\left(\sum_{i=1}^{N}h_i^{\,2}\,w^2(h_i)\right)\left(\sum_{i=1}^{N}\frac{h_i^{\,4}}{4}w^2(h_i)\right)-\left(\sum_{i=1}^{N}\frac{h_i^{\,3}}{2}w^2(h_i)\right)^2} \tag{A-13}$$